IUN

THIS

MEN

RE

LA-UR -82-342

Conf-820705--2

MASTER

Los Alamos National Laboratory is operated by the University of California for the United States Department of Energy under contract W-7405-ENG-36

LA-UR--82-342

DE82 008124

TITLE: PREDICTION OF FAILURE MODES FOR CONCRETE NUCLEAR-CONTAINMENT BUILDINGS

AUTHOR(S): Thomas A. Butler

SUBMITTED TO: ASME/ANS Nuclear Engineering Conference,
Portland, Oregon, July 25-28, 1982

Los Alamos Los Alamos National Laboratory
Los Alamos, New Mexico 87545

PREDICTION OF FAILURE MODES FOR CONCRETE NUCLEAR-CONTAINMENT BUILDINGS

by

T. A. Butler
Los Alamos National Laboratory
Los Alamos, New Mexico 87545

ABSTRACT

The failure modes and associated failure pressures for two common generic types of PWR containments are predicted. One building type is a lightly reinforced, posttensioned structure represented by the Zion nuclear reactor containment. The other is the normally reinforced Indian Point containment. Two-dimensional models of the buildings developed using the finite element method are used to predict the failure modes and failure pressures. Predicted failure modes for both containments involve loss of structural integrity at the intersection of the cylindrical sidewall with the base slab.

I. INTRODUCTION

During a postulated severe accident in a pressurized water reactor (PWR) loss of both natural convection cooling and the emergency cooling system could lead to reactor core dryout, heat up, and eventual meltdown. This will subsequently lead to generation of steam and noncondensible gases that could conceivably raise the internal pressure of the PWR containment building enough to cause it to fail. Because the containment building is the last line of defense in protecting the public from a release of fission products, the ultimate pressure capacity of the building becomes an important input to analysis of the consequences of core-melt accidents. In this report we address the question of ultimate containment capability under quasistatic overpressurization for the Indian Point and Zion nuclear reactors.

Previous studies performed by Sandia National Laboratories (SNL) on Indian Point[1] and Los Alamos National Laboratory on Zion[2] concluded that the failure mode for both buildings was excessive hoop strain in the cylindrical sidewall. Independent analyses performed by the utilities were in good agreement with conclusions drawn by SNL and Los Alamos. Because of the time frame involved, these initial studies left out considerable detail and used several

assumptions that weren't necessarily correct. Both of these studies used design material properties. In the current work we developed more detailed models of both buildings and used as-built material properties for the critical structural components.

The specific buildings modeled were the Zion Unit No. 2 containment and the Indian Point Unit No. 3 containment. Applied loads from internal pressure, weight of structure and equipment, and, for the Zion building, posttensioning loads were included. The scope of this study does not include response to loads induced from thermal gradients. A more detailed description of the response of these buildings to accident loads is presented in Ref. 3.

II. CONTAINMENT BUILDING DESIGN

The Zion containment building is a lightly reinforced, posttensioned concrete structure with the basic dimensions and features shown in Fig. 1. Vertical posttensioning in the cylindrical sidewall is provided by 216 steel tendons anchored at the base slab on the bottom and the transition ring on the top. Posttensioning in the hoop direction is provided by 579 tendons that each span 120^{o}. These are anchored in six vertical buttresses equally spaced around the building. The dome is posttensioned by three groups of 63 tendons each, oriented at 120^{o} with respect to each other. These tendons anchor on the outside vertical face of the cylinder-dome transition ring. All tendons are made of ninety-0.25 in.-(6 mm)-diam steel wires with a combined ultimate capacity of ~ 240 000 psi (1660 MPa). When the building is constructed, the tendons are stressed to 80% of their ultimate capability. Because of creep of the compressed concrete, the tendon stress gradually drops to 60-65% of the ultimate capability where it stays during the remaining life of the structure.

Figure 2 shows details of the tendon anchorages at the intersection of the cylindrical sidewall with the base slab. This figure also shows the steel reinforcement pattern at the intersection for counteracting the high shear and moment that is experienced. The intersection of the cylindrical sidewall with the dome transition ring also experiences discontinuity loads and, therefore, has a similar design.

A 0.25 in.-(6.4 mm)-thick steel plate made of ASTM A442 Grade 60 carbon steel lines the entire inner face of the containment. This leak-tight membrane has a nominal elongation of 23% in 2 in., so the concrete to which it is

anchored will have to crack conside ably and the associated steel reinforcement will have to yield to allow the liner to stretch enough to fail.

The Indian int containment building is a reinforced concrete right vertical cylinder w 'h a hemispherical dome and has the basic dimensions and features shown in Fig. 3. The only location in the structure where significant shear and moment loads develop during quasistatic pressurization is at the intersection of the cylindrical sidewall with the basemat. Additional steel reinforcement in this area consists of bent bars and stirrups for increasing the shear capability.

The steel liner for the Indian Point building is constructed of ASTM A442 Grade 60 carbon steel. Its thickness is 0.25 in. (6.4 mm) on the containment floor and 0.50 in. (12.7 mm) on the lower portion of the cylindrical sidewall. On the upper portion of the cylindrical sidewall and inside hemispherical dome it is 0.38 in. (9.5 mm) thick.

III. STRUCTURAL MODELING

Both the Zion and Indian Point containment buildings are basically axisymmetric structures so two-dimensional axisymmetric finite element models were used to determine their failure modes and associated failure pressures. The ADINA finite element code[4] was used to develop the two-dimensional models. It includes a good concrete constitutive model and the Los Alamos version of the code has a nonlinear, two-dimensional shell finite element for simulating the containment liners. The two-dimensional mesh generated for representing the Zion containment building is shown in Fig. 4. Mesh density was chosen to give good resolution of stresses in high moment and shear areas and to place nodal points to which the liner is attached at the approximate actual liner anchor spacing. The mesh for the Indian Point containment building is similar.

Under the base slab we included nonlinear springs to simulate the restraining effect of the ground on downward motion. These springs are very stiff in compression and have no stiffness in tension. This allows the buildings' base slabs to uplift with no boundary restraint. We neglected the effect of soil on the outside of the lower portion of the cylindrical sidewall for both buildings. Comparisons with structural integrity tests indicate that this is a good approximation (Sec. V).

The concrete material model used is the tensile-cracking, compression-crushing, strain-softening model described in Ref. 5. The tensile cracking

mechanism is implemented by examining the maximum principal stress at each element integration point. If this stress exceeds the uniaxial cutoff tensile stress, a failure plane (interpreted here as a "cracked" plane) has formed normal to the maximum principal stress direction. The normal stiffness across this plane is decreased to a user-specified factor times the original stiffness. The shear stiffness at this integration point is similarly reduced. We used the 8-node isoparametric axisymmetric element with a 3 by 3 array of integration points. A normal stiffness reduction factor of 0.000 1 and a shear stiffness reduction factor of 0.5 was used.

Steel reinforcement for both buildings has a nominal yield strength of 60 000 psi (414 MPa). All hoop reinforcement is represented with ring finite elements. The appropriate area for each element was determined by integrating along the meridional direction using the two-dimensional continuum element shape functions. Meridional reinforcement was represented with two-node truss elements. The cross-sectional area was determined by the amount of reinforcement at a certain radial/vertical location in a one radian segment of the structure. This method of representing the steel reinforcement assumes a perfect bond with the concrete at node points. However, between node points, displacement compatibility between the concrete and truss elements does not exist. Representative reinforcement placement in the finite element grids is shown in Fig. 4. We did not directly include the effect of reinforcement ties or stirrups in either model. However the effect of this additional reinforcement was indirectly included by retaining a significant amount of shear stiffness after cracks develop.

The tendons in the Zion building were also represented with ring and truss elements and were given an initial strain of 0.005 2. The axial stress in the tendon elements after posttensioning was predicted to be from about 140 000 psi (0.97 GPa) to 150 000 psi (1.03 GPa), which is 58-63% of their ultimate strength and is consistent with design assumptions used in the Zion structure.

The steel liner plates were modeled with a three-node axisymmetric shell element. Each element had four integration points along the meridional direction and one through the thickness. For all three steel components, reinforcement, tendons, and liners, we used a value for Young's modulus in the elastic region of 29×10^6 psi (200 GPa). Yield strengths were based on as-build material properties. Tangent moduli were set at 0.001% of Young's modulus. This essentially gives an elastic perfectly-plastic representation of all the steel components.

IV. COMPARISON WITH STRUCTURAL INTEGRITY TESTS

The two-dimensional analytical models of both containment buildings were loaded with appropriate internal pressures to compare their predicted displacements and concrete crack patterns with those measured during the Structural Integrity Tests (SITs). For both tests the buildings were slowly pressurized to 54 psig (0.37 MPa) internal pressure, which is 115% of the design pressure. Pressurization was held constant at selected internal pressures to enable mapping of crack patterns. Throughout the time of the tests invar wire extensometers were used to measure relative displacement at several locations. Results of the SITs are presented in detail in Ref. 6 for the Zion containment building and in Ref. 7 for the Indian Point Containment building.

The Zion containment building finite element model was loaded first with the dead weight of the building and internal structure and equipment along with the tendon preload. This load state represents the initial condition configuration of the building before the SIT. Next, an internal pressure of 54 psig (0.37 MPa) was applied to the model. Load step increments were not necessary because the model predicts essentially linear behavior up to this pressure. Figure 6 shows the locations of extensometers used to measure radial displacement of the sidewall and vertical displacement of the dome for the Zion containment building. Table I shows predicted and measured displacements for selected gauge locations. The model predictions are generally very close to the measured displacements. The largest predicted error is at the base of the cylindrical wall where the displacement is quite small. The larger than predicted displacement in this area does indicate a negligible effect from the soil surrounding the base of the building.

A visual crack survey was performed before the SIT and at the maximum test pressure. Several fine cracks representative of those typically present from the thermal and drying shrinkage were observed before the test with no additional cracks being observed at an internal pressure of 54 psig. The analytical model predicts some tensile cracks on the outer surface of the structure at the dome transition ring after posttensioning with no internal pressure. When the building is pressurized to the maximum test pressure of 54 psig (0.37 MPa), the only additional cracking that occurs is under the basemat where it could not have been observed during the SIT. Basemat cracking is caused by uplift and is minimal at test pressures.

Because considerable cracking of concrete occurs in the Indian Point containment building during the SIT, the finite element model developed to predict its response was loaded incrementally. For convenience in comparing analytical results with test data, we loaded the structure in increments that generated response predictions at 12 psig (0.08 MPa), 21 psig (0.14 MPa), 42 psig (0.29 MPa), and 54 psig (0.37 MPa). Prior to applying the pressure loads the dead weight of the building along with internal structures and equipment was applied to generate the proper initial conditions. Table II shows predicted and measured displacements for selected gauge locations at 54 psig (0.37 MPa) internal pressure. Because this building was loaded incrementally, we have shown a representative comparison of analytical predictions with measured values as a function of pressure during the SIT in Fig. 6 where displacement of the dome apex is shown.

TABLE I
COMPARISON OF PREDICTED AND MEASURED SIT RESULTS
FOR THE ZION CONTAINMENT BUILDING

Gauge	Measured	Predicted	Deviation
	Radial Displacement of Cylinder Wall		
H1	0.07 in. (18 mm)	0.03 in. (8 mm)	+0.04 in. (10 mm)
H2	0.18 in. (46 mm)	0.15 in. (38 mm)	+0.03 in. (8 mm)
H3	0.14 in. (36 mm)	0.14 in. (36 mm)	0.00
H4	0.14 in. (36 mm)	0.14 in. (36 mm)	0.00
H5	0.05 in. (13 mm)	0.05 in. (13 mm)	0.00
	Vertical Displacement of Dome		
D1	0.38 in. (96 mm)	0.36 in. (91 mm)	+0.02 in. (5 mm)
D2	0.42 in. (107 mm)	0.35 in. (89 mm)	+0.07 in. (18 mm)
D3	0.21 in. (53 mm)	0.20 in. (51 mm)	+0.01 in. (3 mm)

Note: Positive deviation indicates the measured displacement is greater than the predicted response.

For this containment building the calculated displacements are all greater than those measured during the SIT. The principal cause for the deviations in the displacements is the way concrete cracking is handled in the analytical model. For example, when a crack occurs perpendicular to the hoop direction in the model, the stiffness contribution from the concrete in the hoop direction is reduced to 1% of its original value. This simulates a very close spacing of cracks. Crack surveys taken during the SIT indicate crack spacing on the order of 1-3 ft (0.30-0.91 m). This means that, even though cracked, the concrete, because of crack spacing and bond to rebar, still contributes significantly to the overall stiffness. As strain in the rebar and concrete cracking increase, more loss of bond will occur and the model predictions become less conservative.

TABLE II

COMPARISON OF PREDICTED AND MEASURED SIT RESULTS
FOR THE INDIAN POINT CONTAINMENT BUILDINGS

Point	Elevation	Measured (Point #)	Prediction	Deviation
		Radial Displacement of Cylinder Wall		
3	56.5 ft (17.2 m)	0.274 in. (69.6 mm)	0.389 in. (98.8 mm)	-0.115 in. (29.2 mm)
1	91 ft (27.7 m)	0.634 in. (161.1 mm)	0.729 in. (185.0 mm)	-0.075 in. (19.1 mm)
18	111 ft (33.8 m)	0.557 in. (144.5 mm)	0.707 in. (179.6 mm)	-0.150 in. (38.1 mm)
[illegible]	131 ft (39.9 m)	0.578 in. (146.8 mm)	0.699 in. (177.5 mm)	-0.121 in. (30.7 mm)
[illegible]	151 ft (46.0 m)		0.710 in. (180.3 mm)	
4	171 ft (52.1 m)	0.675 in. (171.5 mm)	0.706 in. (179.3 mm)	-0.031 in. (7.9 mm)
0	191 ft (58.2 m)	0.461 in. (117.1 mm)	0.603 in. (153.2 mm)	-0.142 in. (36.1 mm)
		Vertical Displacement of Dome		
31	191 ft (58.2 m)	0.344 in. (84.8 mm)	0.419 in. (106.4 mm)	-0.065 in. (21.6 mm)
2	256.5 ft (78.2 m)	0.586 in. (148.7 mm)	0.667 in. (169.4 mm)	-0.081 in. (20.6 mm)

Note: Positive deviation indicates the measured displacement is greater than the predicted response.

V. CONTAINMENT STATIC RESPONSE AND FAILURE

The two-dimensional analytical models of the containment buildings were incrementally loaded to determine their respective failure pressures and failure modes. Load increments were first chosen to provide a good representation

of structural response as a function of internal pressure. As the structures approached failure, the increments were necessarily decreased sig ficantly to obtain proper convergence.

Because the structures undergo step changes in stiffness when concrete cracks open and close, the modified Newton-Raphson solution method with equilibrium iteration that is normally used in the ADINA code could not be effectively applied. Instead, we held the pressure at one value for ten to twenty load steps reforming the stiffness matrix after each step. No equilibrium iterations were used. Convergence was determined by following the displacement of three critical points; these were at the midheight of the cylindrical sidewall, at the apex of the dome, and at the outer corner of the basemat. When all three points converged on unique values the pressure was incremented. This procedure is equivalent to a full Newton-Raphson method with iterations but no equilibrium checks.

Figure 7 shows the loading history used in the analysis of the Zion building. It should be remembered that several iterations are involved in each load step shown. Concrete cracking remains essentially unchanged between the maximum SIT pressure of 54 psig (0.37 MPa) and 85 psig (0.59 MPa). At an internal pressure of 85 psig (0.59 MPa) considerable cracking occurs on the inside of the cylindrical wall at its intersection with the basemat and on the inside of the transition ring. These cracks are from tensile stresses in the meridional direction caused by the bending moments generated at these structural discontinuities. The complete midsection of the cylindrical sidewall cracks perpendicular to the hoop direction at 95 psig (0.66 MPa). Additional cracking at the base of the cylindrical wall from the large shear stresses also occurs at this pressure. Between 100 psig (0.69 MPa) and 105 psig (0.72 MPa) internal pressure the dome cracks perpendicular to the hoop direction.

Displacements of the building were successfully calculated for an internal pressure of 125 psig (0.86 MPa). The displaced shape of the structure is shown in Fig. 8 where the displacements have been amplified by a factor of 50 to make the shape easier to visualize. Of particular importance are the base slab uplift and the high moment and shear at the base of the cylindrical wall. At this internal pressure the concrete has cracked considerably throughout the structure. However, the steel reinforcement and posttensioning tendons remain elastic except near the apex of the dome where this axisymmetric model does not adequately represent the strength of the actual building. Because of that

state of stress, structural failure was not expected for small increments in internal pressure. However, an increment of only 0.5 psi (3540 Pa) results in a stress state where displacements become very large and convergence cannot be obtained. This indicates that the building has reached a structural instability and increasing displacements can be expected even with decreasing internal pressure.

The most highly-stressed portion of the structure at this point (125 psig (0.86 MPa) internal pressure) is in the base of the cylindrical wall. Here the high moment and shear loads from the bending of the wall are amplified by the doming of the base slab. At 85 psig (0.59 MPa) internal pressure the concrete begins cracking on the inside of the wall in this region. At the base of the wall the cracks are caused by the combined action of the tensile bending and shear stresses. Even after cracking, the concrete maintains a considerable amount of shear-carrying capability because the reinforcement has not yielded. With the ADINA code we allow the concrete to carry only 0.01% of its original tensile capability and 50% of its original shear capability after cracking occurs. As internal pressure increases and shear stresses build, additional cracking occurs perpendicular to the initial cracks. This starts at the inside of the wall and proceeds toward the outside. When this happens the concrete should no longer have any shear-carrying capability. However, because of code limitations, the analytical model still considers 50% of the original shear stiffness to be present. To insure that this phenomena does not mask a failure below 125 psig (0.86 MPa) we checked the structure by determining that the steel in this area can absorb the shear carried in the concrete without yielding at 125 psig (0.86 MPa) internal pressure. Extrapolation to determine where the steel would yield is not possible because of the complexity of the stress distribution.

If the instability at 125 psig (0.86 MPa) internal pressure is only a numerical artifice and the building can actually take more pressure, we can estimate the pressure for other possible failure modes. In particular, the failure mode predicted in previous studies[2] involving yielding of rebar and tendons in the hoop direction in the cylindrical wall is estimated to occur at 136.4 psig (0.94 MPa) internal pressure. This is within 1 psig (6895 Pa) of the capability of the wall based on limit analysis.

Figure 9 shows the displacements of two points on the structure as a function of pressure. Radial displacement at the midheight of the cylindrical

sidewall is linear until the concrete cracks perpendicular to the hoop direction at 85 psig (0.59 MPa) internal pressure. It remains essentially linear with increased slope after cracking is complete at 95 psig (0.66 MPa) to the maximum pressure attained. Vertical displacement of the dome apex changes slope more gradually as general concrete cracking from meridional stresses begins near the top of the building and gradually moves down, because of gravity, to involve the complete sidewall.

Hoop strain in the steel liner at the midheight of the cylindrical sidewall follows the same pattern as wall displacement and does not exceed 0.2% before 125 psig (0.86 MPa) internal pressure. Meridional strain at the base of the sidewall becomes quite large (0.6%) in a very localized area in the conical section of the liner that acts as a transition between the horizontal floor and sloping section of the sidewall (Fig. 2). The liner in the sidewall immediately above this area experiences a maximum strain of 0.15%. The initial strain state of the liner is important in predicting its response. In the model used for this study, initial compression of the liner from gravity and posttensioning is accounted for. However, additional compressive strains expected from creep effects are not present.

Response of the Indian Point containment building is much more straightforward than that of the Zion building because it is not posttensioned. The loading history used for analyzing the Indian Point building is similar to that used for the Zion building. As discussed in the preceeding section of the report, the containment building experiences considerable concrete cracking at SIT pressures. As the internal pressure increases concrete cracking becomes more widespread, especially at the intersection of the cylindrical sidewall and basemat, which is the predicted failure point. At 54 psig (0.37 MPa) internal pressure the base of the cylindrical wall is cracked perpendicular to the meridional direction from combined tensile and shear forces. Additional cracks perpendicular to these begin appearing at the base of the sidewall on the inside surface at 70 psig (0.48 MPa). When this occurs, the concrete begins losing its capability to carry shear (see earlier discussion for the Zion building). At 118 psig (0.81 MPa) internal pressure the shear failure in the concrete has progressed 75% of the way through the wall. In addition, concrete on the outside of the wall has begun to crush from the high compressive loads. Any additional pressure results in additional crushing and failure to numerically converge

Figure 10 shows the stress in the shear reinforcement at the base of the wall. As concrete cracking progresses through the wall and it is able to carry less shear, the stress in this reinforcement increases more rapidly with pressure. A partially offsetting effect is that, as the concrete cracks and crushes at this location, the moment at the intersection is reduced. Then the shear carried at the lower end of the wall is decreased somewhat. The sum of these two effects produces the curve shown in the figure. The sharp change in slope at 110 psig (0.76 MPa) internal pressure occurs when the concrete begins crushing in the outside of the wall. At 118 psig (0.81 MPa) internal pressure the stress in the shear reinforcement has reached 90% of its yield stress. Linear extrapolation of this curve indicates shear reinforcement yielding at 120 psig (0.83 MPa) internal pressure.

If the concrete carries no shear and the maximum shear force possible is developed at this intersection, simple handbook calculations show that the shear reinforcement would yield at ~ 112 psig (0.77 MPa) internal pressure. In reality, because the shear force at the joint decreases as the concrete fails, the failure pressure should be somewhat higher. Because of the highly complex and nonlinear nature of the structural behavior at this joint, we are constrained to rely on the predictions of the analytical model. It predicts failure at 118 psig (0.81 MPa) internal pressure from excess concrete cracking and crushing coupled with a loss of shear carrying capability at the base of the cylindrical wall.

Meridional reinforcement at the inside of the cylindrical sidewall at its intersection with the base mat yields at ~ 105 psig (0.72 MPa) internal pressure. The liner yields at 96 psig (0.66 MPa) internal pressure. However, its strain increases much more rapidly after 105 psig when the inner meridional reinforcement yields. At 118 psig (0.81 MPa) internal pressure the strain in the liner in the hoop direction in the cylindrical wall is approximately 0.2%, which indicates yield but not failure.

VII. CONCLUSIONS

Results of our quasistatic analysis of both containment buildings are summarized in Table 1. The apparent failure mode for the Zion containment building is loss of overall structural integrity in the high shear and moment regions at the base of the cylindrical sidewall. This occurs at 125 psig

(0.86 MPa) internal pressure. The Indian Point containment building is predicted to fail at the base of its cylindrical sidewall at an internal pressure of 118 psig (0.81 MPa). It is difficult to calculate error bounds for these failure pressures because of the complex failure mode involving shear failure of concrete. However, we can predict accurate upper bounds on failure pressures because, for both buildings, these involve membrane failure of the cylindrical sidewalls in the hoop direction. A simple limit analysis using as-built material properties was used to obtain the values presented in Table III.

TABLE III

SUMMARY OF QUASISTATIC ANALYSES

ZION	
First concrete cracking	85 psig (0.59 MPa)
First reinforcement yield	None
Liner first exceeds 0.3% strain	117 psig (0.81 MPa)
Predicted failure pressure	125 psig (0.86 MPa)
Lower bound failure pressure	105 psig (0.72 MPa)
Upper bound failure pressure	134 psig (0.92 MPa)
INDIAN POINT	
First concrete cracking	30 psig (0.21 MPa)
First reinforcement yield	100 psig (0.69 MPa)
Liner first exceeds 0.3% strain	105 psig (0.72 MPa)
Predicted failure pressure	118 psig (0.81 MPa)
Lower bound failure pressure	112 psig (0.77 MPa)
Upper bound failure pressure	133 psig (0.92 MPa)

The lower bound failure pressure given in Table III for the Zion building is very conservative and is simply based on the pressure at which more than half of the concrete at the base of the cylindrical sidewall is predicted to lose its shear carrying capability. A limit analysis of the shear carrying

capability of the base of the cylindrical sidewall for the Indian Point building gives its lower bound failure pressure. This is also conservative because we assume an uncracked sidewall in determining the shear force acting at this point.

REFERENCES:

1. "Report on the Zion/Indian Point Study, Vol. 1," Sandia National Laboratories report SAND 80-0617, NUREG/CR-1410, 1980.

2. Butler, T. A. and Bennett, J. G., "Nonlinear Response of a Post-Tensioned Concrete Structure to Static and Dynamic Internal Pressure Loads," Computers and Structures, Vol. 13, 1981, pp. 647-659.

3. Butler, T. A. and Fugelso, L. E., "Response of the Zion and Indian Point Containment Buildings to Severe Accident Pressures," Los Alamos National Laboratory report, 1982.

4. Bathe, K. J., "ADINA: A Finite Element Program for Automatic Dynamic Incremental Nonlinear Analysis," Massachusetts Institute of Technology report 82448, September 1975, Revised December 1978.

5. Bathe, K. J. and Ramaswamy, S., "On Three-Dimensional Nonlinear Analysis of Concrete Structures," Nuc. Eng. and Design, Vol. 52, 1979, pp. 385-409.

6. "Structural Response of the Containment Structure of the Zion Nuclear Plant Unit No. 1 During Structural Integrity Tests -- Commonwealth Edison Company," for Sargent and Lundy (submitted by Wiss, Janney, Elstner, and Associates, Inc.), March 1973.

7. "Report on [illegible] Edison's Indian Point Unit No. 3 Containment [illegible] Structural Integrity Test," for [illegible]CO Corporation (prepared by [illegible] Engineers and Constructors Inc.), February, 1975.

FIGURES

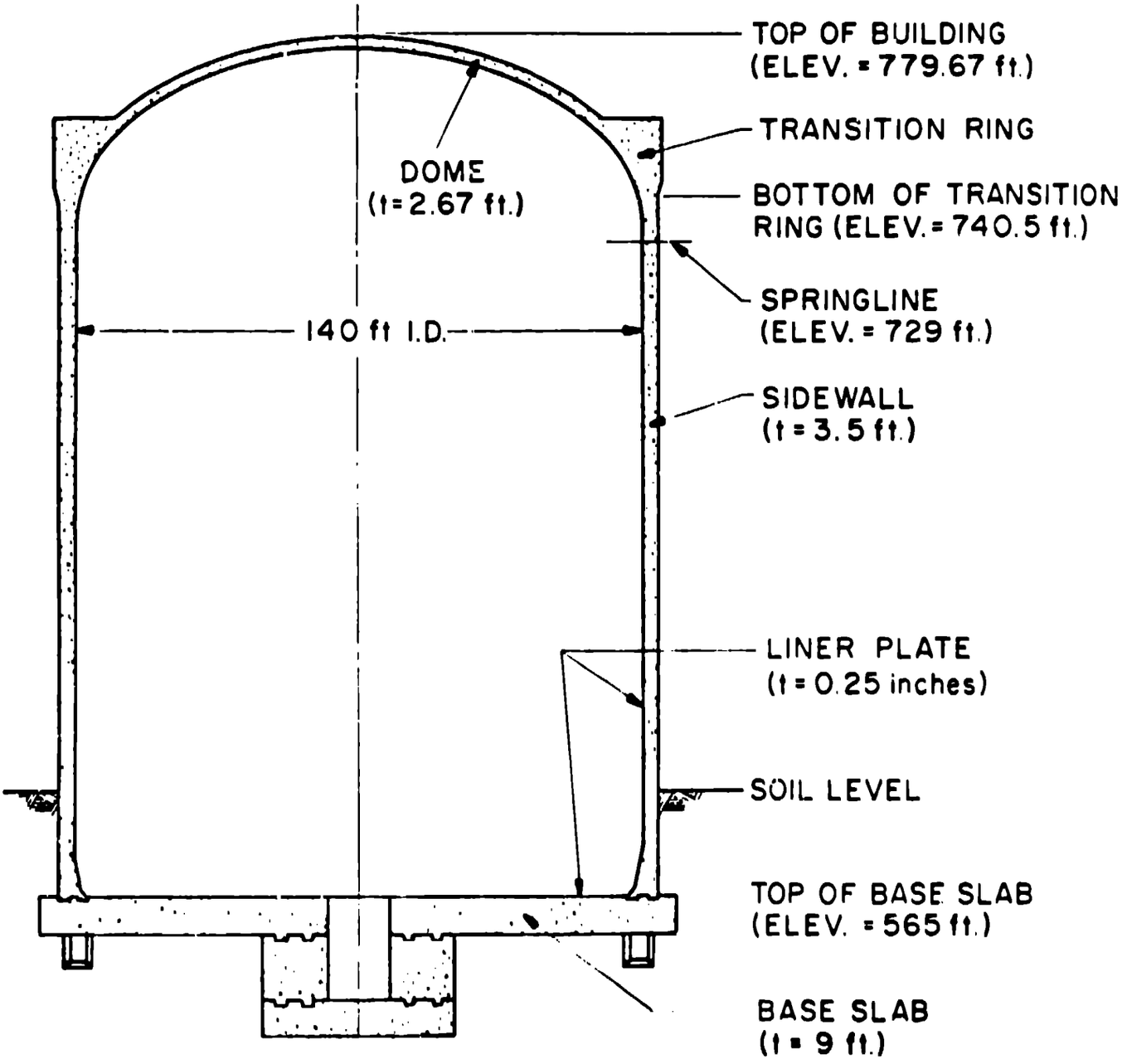
TOP OF BUILDING
(ELEV. = 779.67 ft.)
TRANSITION RING
DOME
(t = 2.67 ft.)
BOTTOM OF TRANSITION
RING (ELEV. = 740.5 ft.)
SPRINGLINE
(ELEV. = 729 ft.)
140 ft I.D.
SIDEWALL
(t = 3.5 ft.)
LINER PLATE
(t = 0.25 inches)
SOIL LEVEL
TOP OF BASE SLAB
(ELEV. = 565 ft.)
BASE SLAB
(t = 9 ft.)

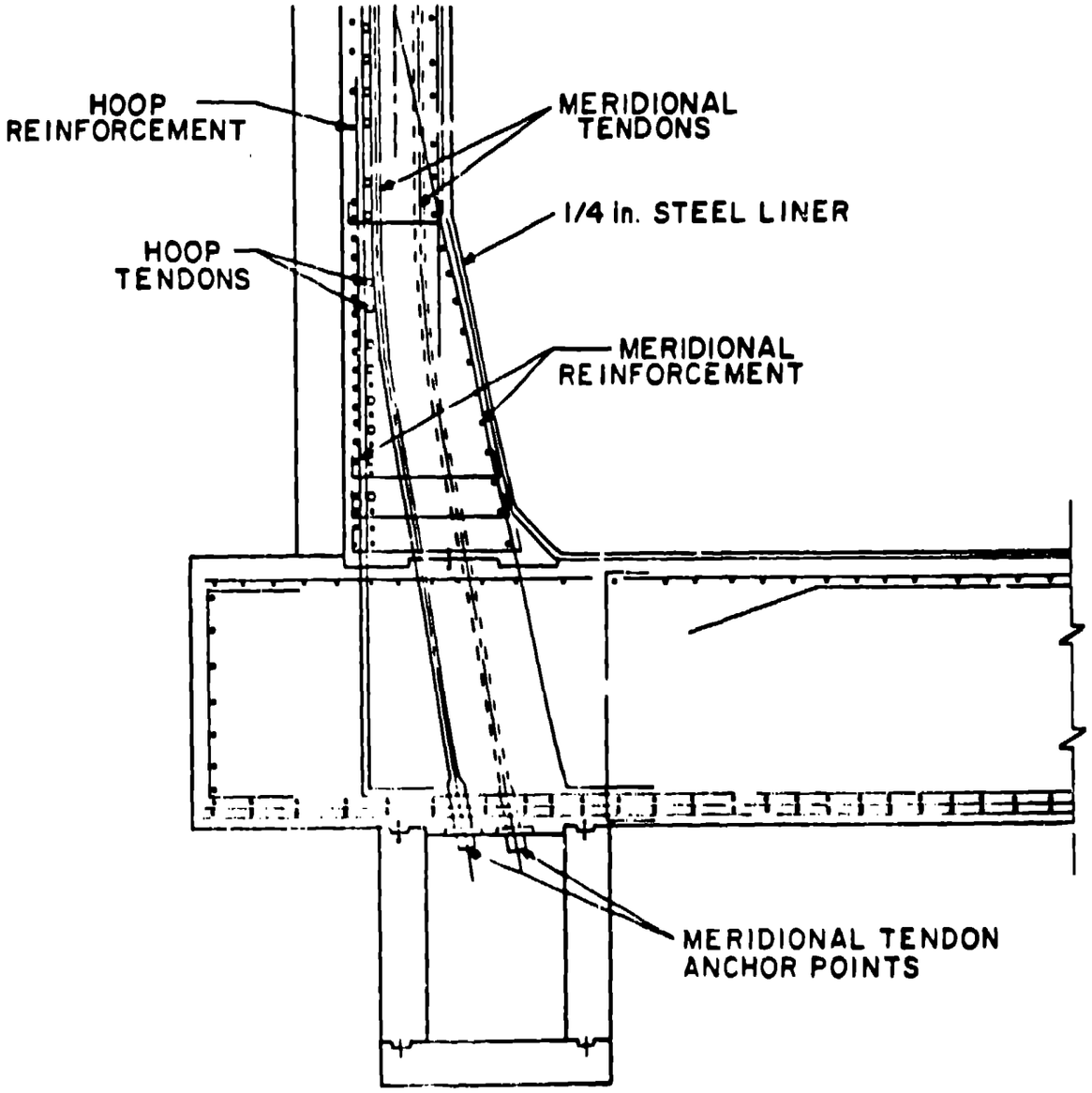
HOOP
REINFORCEMENT
MERIDIONAL
TENDONS
1/4 in. STEEL LINER
HOOP
TENDONS
MERIDIONAL
REINFORCEMENT
MERIDIONAL TENDON
ANCHOR POINTS

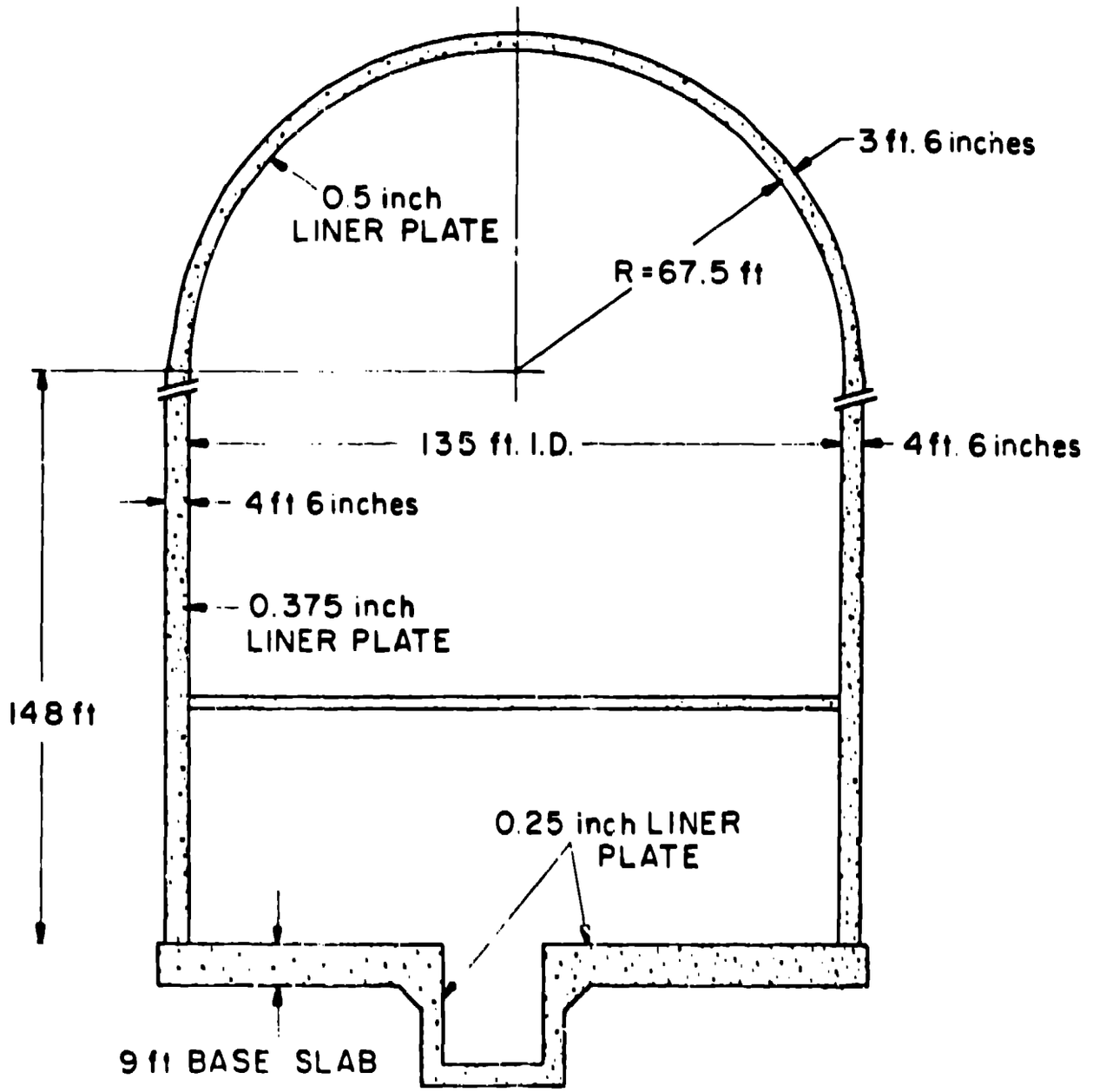
3 ft. 6 inches
0.5 inch
LINER PLATE
R = 67.5 ft
135 ft. I.D.
4 ft. 6 inches
4 ft 6 inches
0.375 inch
LINER PLATE
148 ft
0.25 inch LINER
PLATE
9 ft BASE SLAB

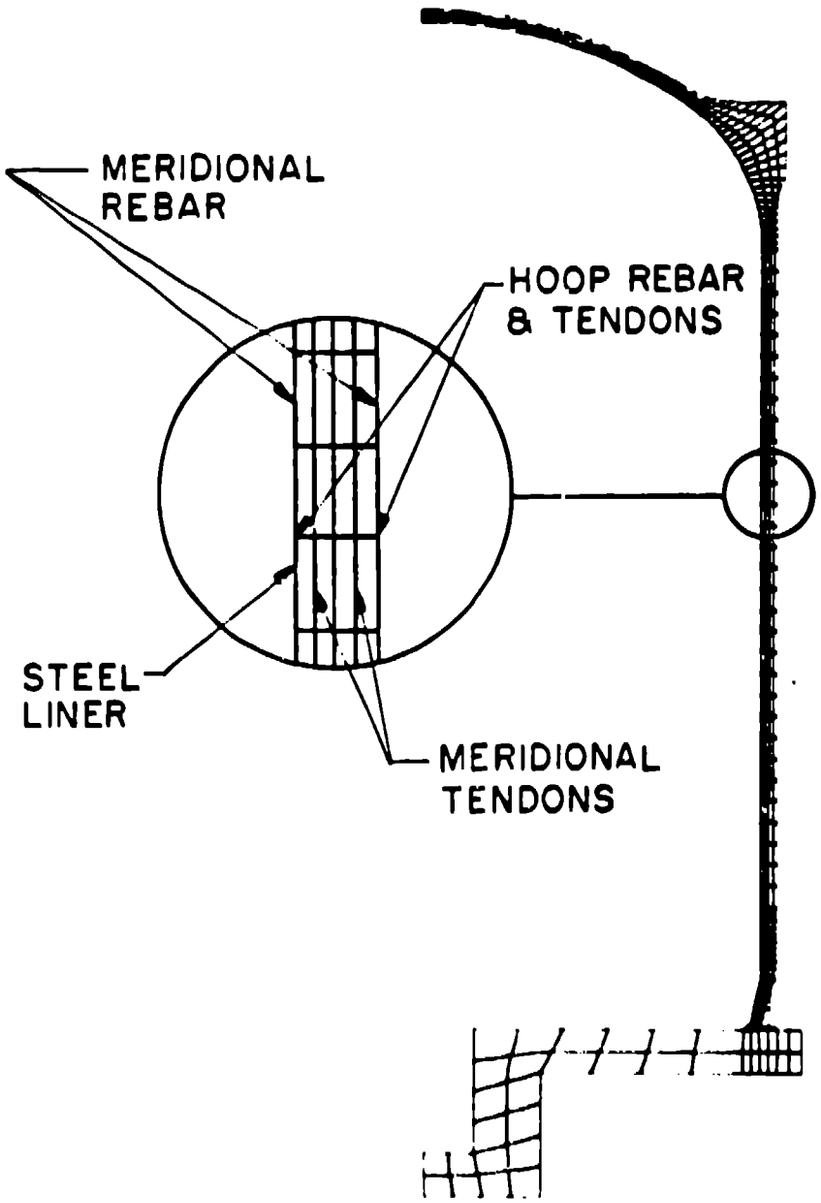
MERIDIONAL
REBAR
HOOP REBAR
& TENDONS
STEEL
LINER
MERIDIONAL
TENDONS

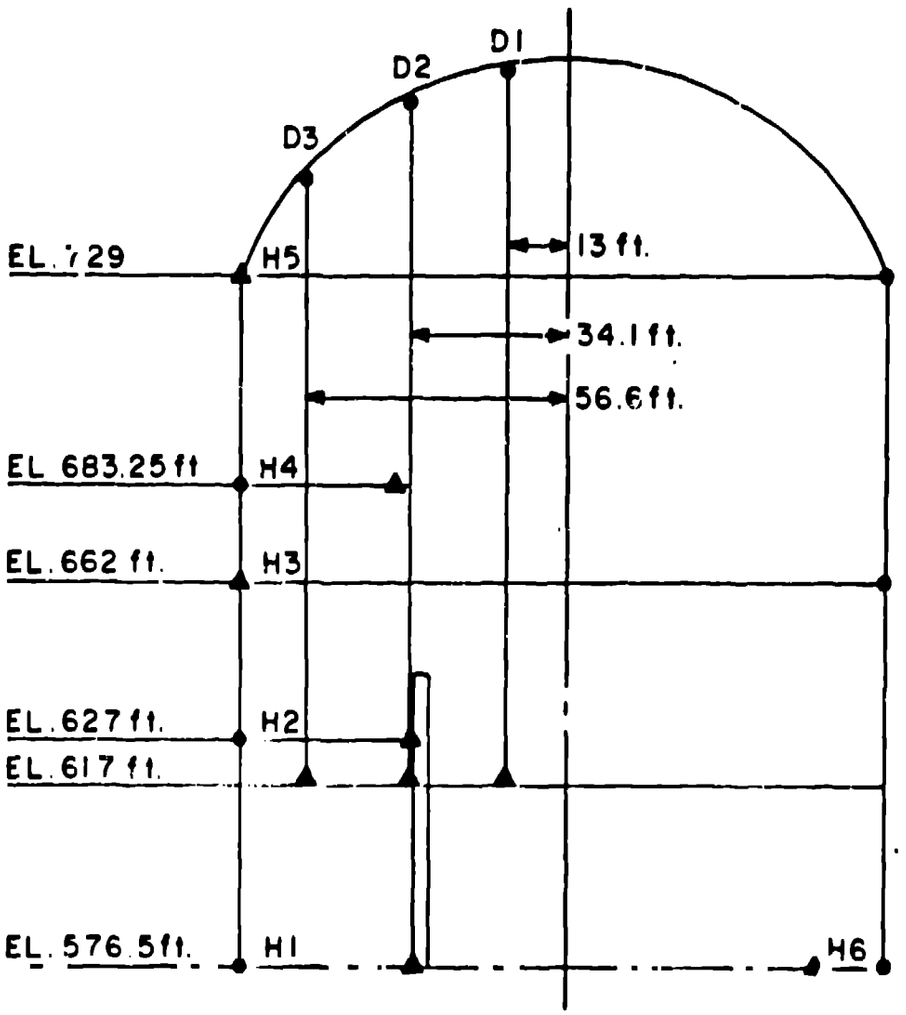
D1
D2
D3
EL. 729
H5
13 ft.
34.1 ft.
56.6 ft.
EL. 683.25 ft
H4
EL. 662 ft.
H3
EL. 627 ft.
H2
EL. 617 ft.
EL. 576.5 ft.
H1
H6
o DEAD END
Δ LIVE END

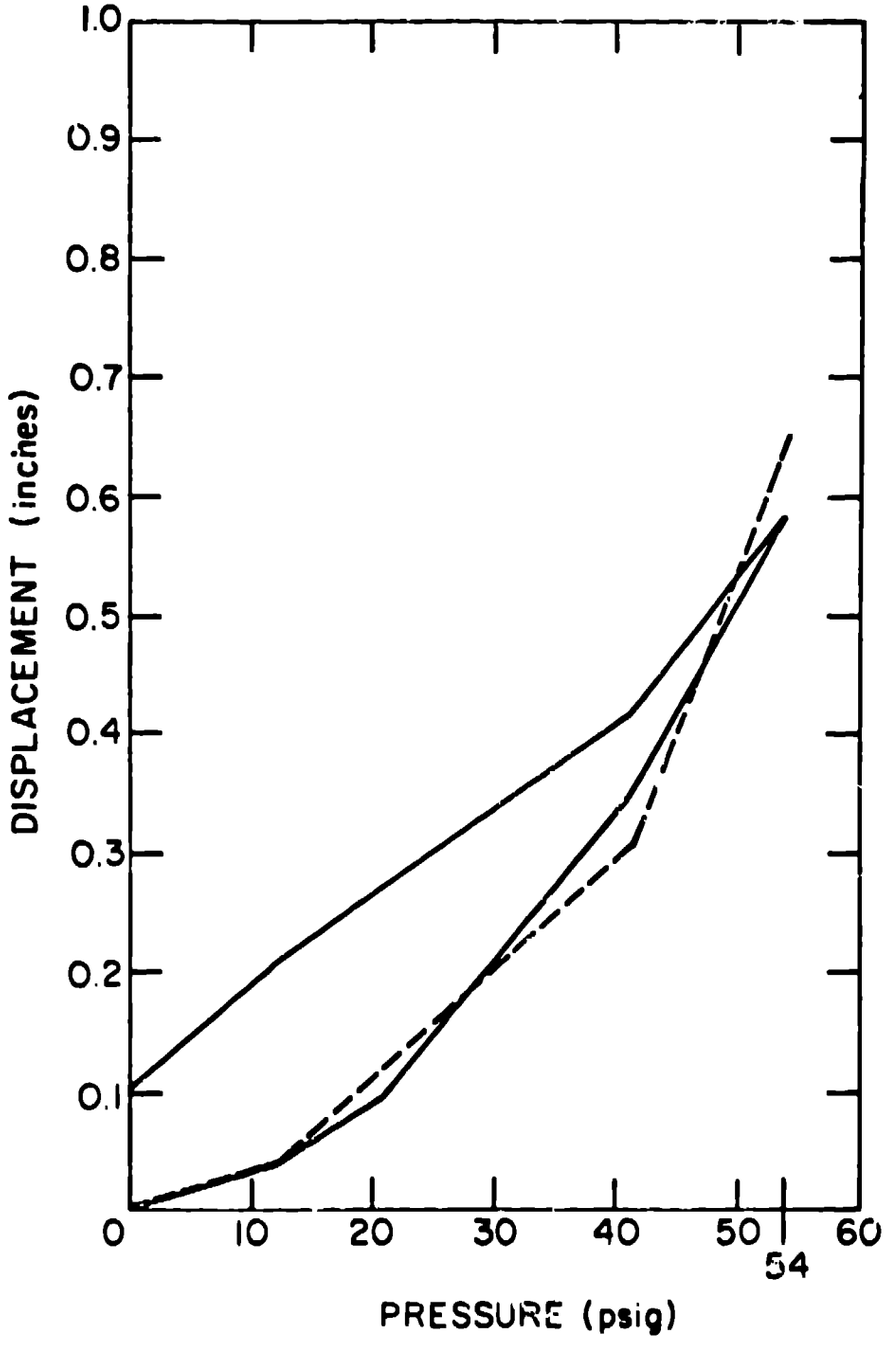
1.0
0.9
0.8
0.7
0.6
0.5
0.4
0.3
0.2
0.1
DISPLACEMENT (inches)
0
10
20
30
40
50
54
60
PRESSURE (psig)

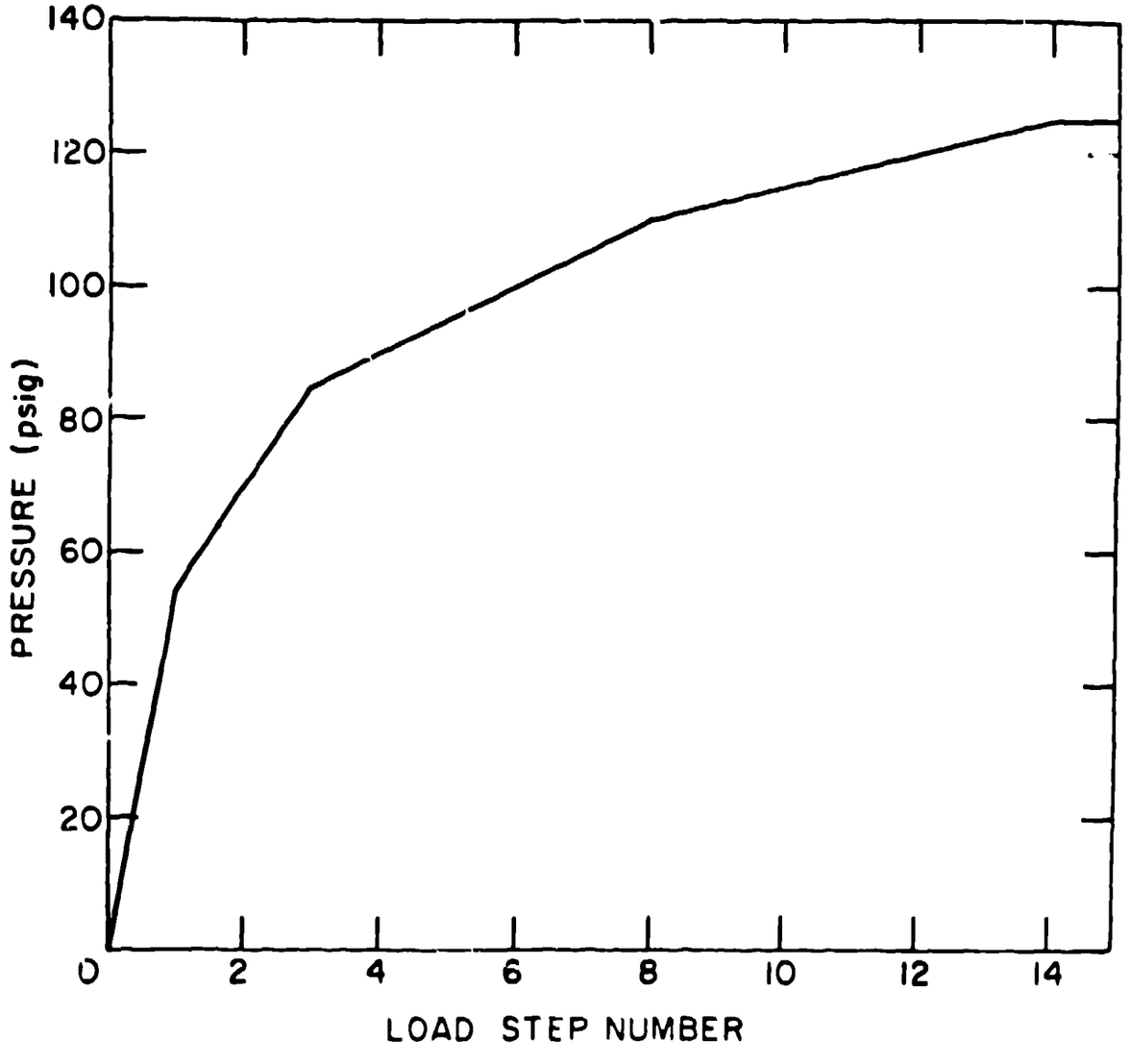
140
120
100
80
60
40
20
0
2
4
6
8
10
12
14
PRESSURE (psig)
LOAD STEP NUMBER

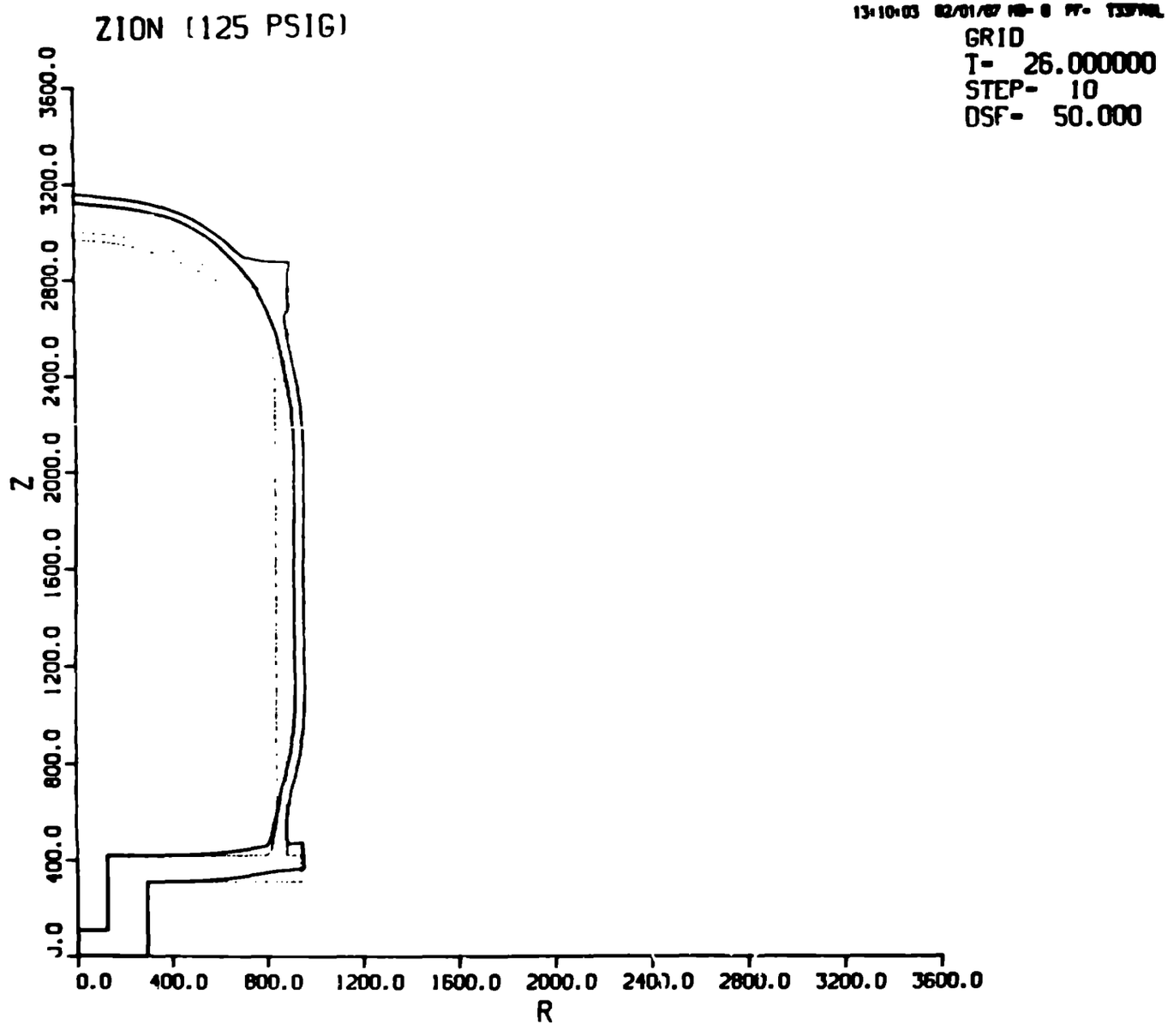
ZION (125 PSIG)
GRID
T= 26.000000
STEP= 10
DSF= 50.000
Z
R
0.0
400.0
800.0
1200.0
1600.0
2000.0
2400.0
2800.0
3200.0
3600.0

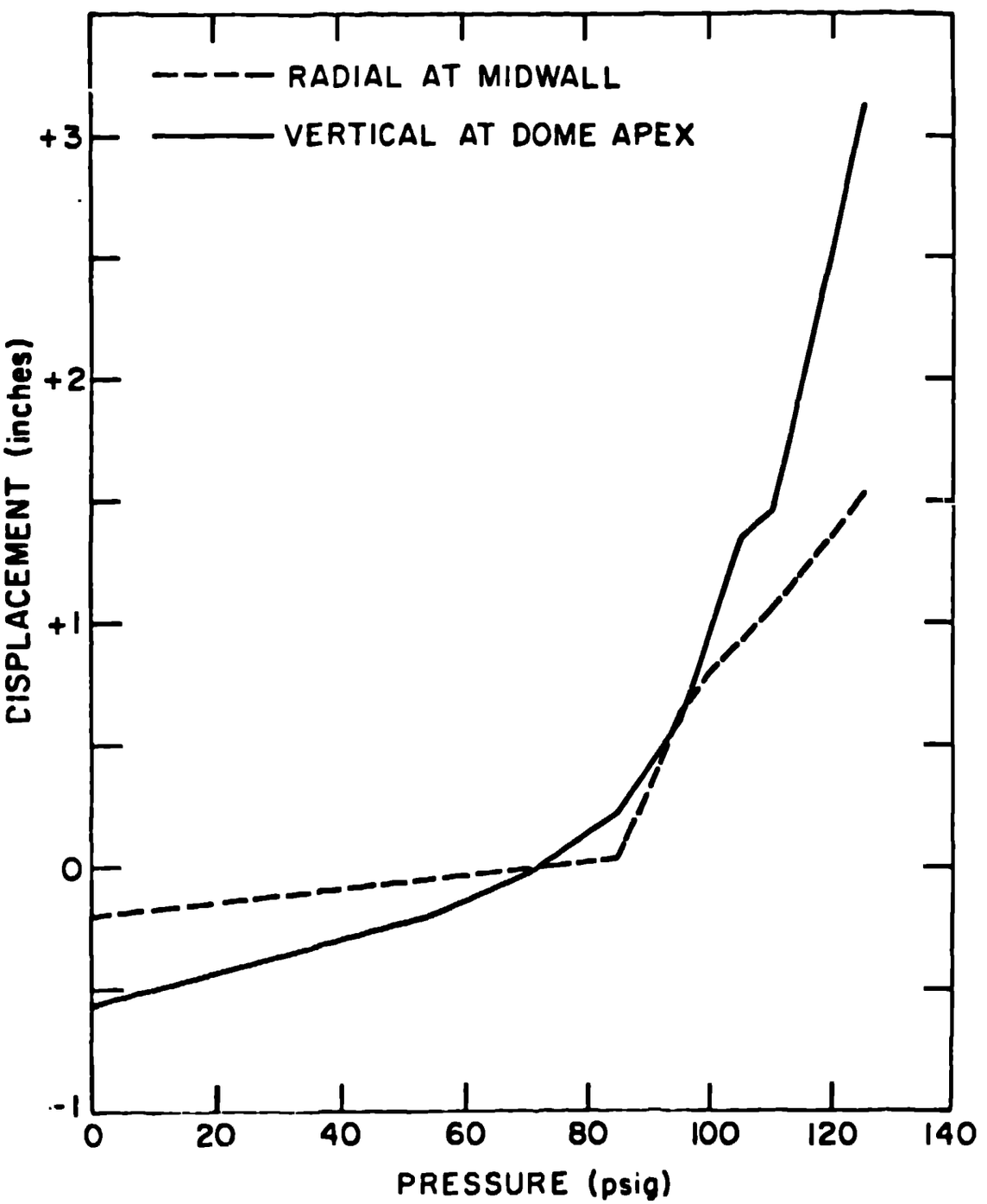
RADIAL AT MIDWALL
VERTICAL AT DOME APEX
+3
+2
+1
0
-1
DISPLACEMENT (inches)
0
20
40
60
80
100
120
140
PRESSURE (psig)

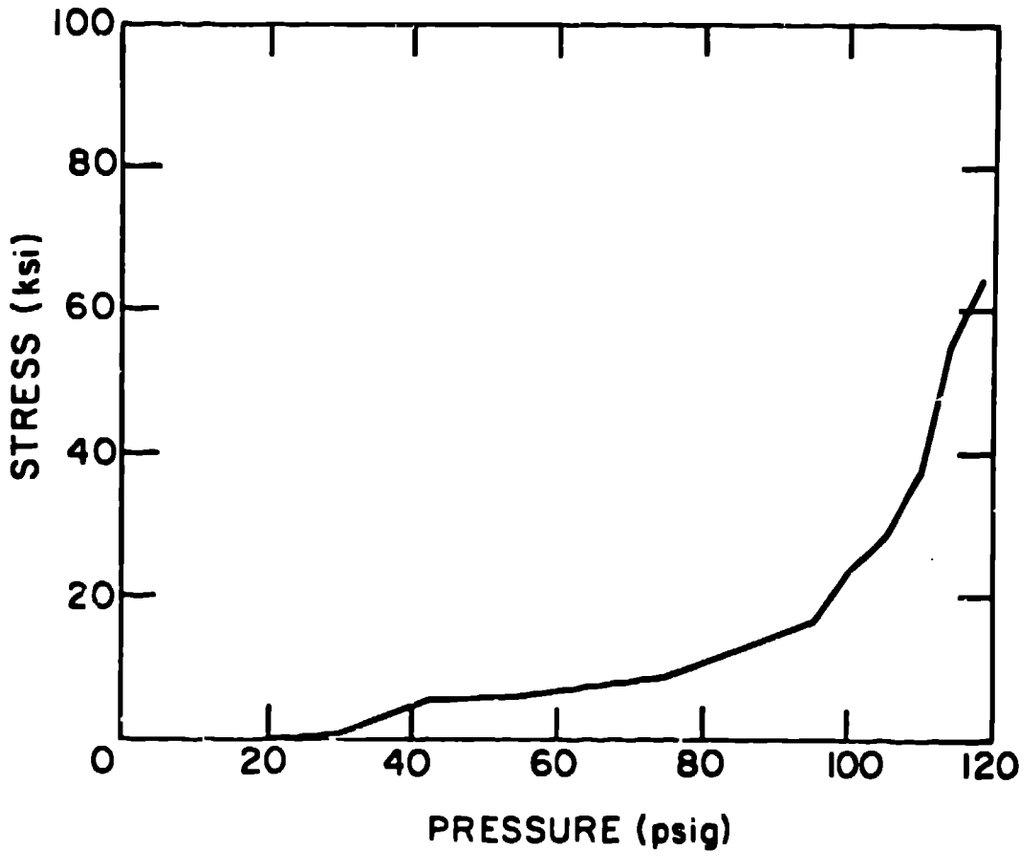
100
80
60
40
20
0
20
40
60
80
100
120
STRESS (ksi)
PRESSURE (psig)